JOURNAL OF NATURAL PRODUCTS

Article

pubs.acs.org/jnp

Tricyclic Polyprenylated Acylphloroglucinols from St John's Wort, *Hypericum perforatum*

Yi Guo,[†] Na Zhang,[†] Chunmei Chen,[†] Jinfeng Huang,[†] Xiao-Nian Li,[‡] Junjun Liu,[†] Hucheng Zhu,[†] Qingyi Tong,[†] Jinwen Zhang,[§] Zengwei Luo,[†] Yongbo Xue,*[,†] and Yonghui Zhang*[,†]

[†]Hubei Key Laboratory of Natural Medicinal Chemistry and Resource Evaluation, School of Pharmacy, Tongji Medical College, and [§]Tongji Hospital Affiliated to Tongji Medical College, Huazhong University of Science and Technology, Wuhan 430030, Hubei, People's Republic of China

[‡]State Key Laboratory of Phytochemistry and Plant Resources in West China, Kunming Institute of Botany, Chinese Academy of Sciences, Kunming 650204, Yunnan, People's Republic of China

Supporting Information

ABSTRACT: The new polyprenylated acylphloroglucinol derivatives **1**−**15** and the known furohyperforin (**16**) were isolated from the stems and leaves of *Hypericum perforatum*. Their structures were determined by analyses of NMR and HRESIMS data. Their absolute configurations were elucidated by a combination of electronic circular dichroism (ECD) and $Rh_2(OCOCF_3)_4$-induced ECD, as well as X-ray diffraction crystallography. The new hyperforatin F (**9**) contains a unique acetyl functionality at C-1 of the bicyclo[3.3.1]nonane core. Hyperforatins G (**10**) and H (**11**) are similarly the first examples of naturally occurring [3.3.1]-type polycyclic prenylated acylphloroglucinols possessing a carbonyl functionality at C-32. The compounds were tested for their acetylcholinesterase (AChE) inhibitory activities and cytotoxic activities against a panel of human tumor cell lines. Compounds **3**, **5**, **6**, **8**, and **9** exerted moderate inhibitory activities (IC_{50} 3.98−9.13 μM) against AChE.

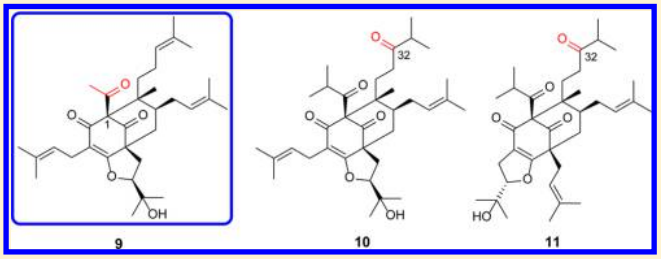

The genus *Hypericum* is one of the largest genera of the family Clusiaceae, comprising 484 species throughout the world.[1] The plants of this genus have been historically used as folk medicines in several regions of the world.[2] The most famous of these plants is *Hypericum perforatum*, also called "St John's wort", which is distributed throughout Asia, North Africa, North America, and Europe.[3] Since the early 1800s, extract of St John's wort (ESJW) has been utilized to attenuate the symptoms of neurological disorders and to heal wounds.[4,5] In addition to the use of ESJW for alleviating mild to moderate depression, which is mainly ascribed to the inhibitory effects of hyperforin on various neurotransmitter receptors,[5,6] further pharmacological investigations have indicated that ESJW exerts versatile biological properties, including antibacterial,[7] antiviral,[8] anti-inflammatory,[9] antioxidant,[10] cytotoxic,[11] and neuroprotective properties.[12] Plants of *H. perforatum* generate various types of secondary metabolites such as phenolic acids, proanthocyanidins, flavonoids, naphthodianthrone, acylphloroglucinols, xanthones, and essential oils.[4] Among them, the prenylated acylphloroglucinols typified by hyperforin have attracted broad interest due to their interesting molecular structures[13] and intriguing pharmacological effects.[14]

During the investigation of structurally interesting and biologically active constituents from the *Hypericum* genus, our group reported the isolation of a variety of new polycyclic prenylated acylphloroglucinols (PPAPs) from *H. sampsonii*, *H. attenuatum*, and *H. ascyron*.[15] Several reports of the biological activities[16] of secondary metabolites, including 26 PPAPs,[3,17,18] from *H. perforatum* were published. The present phytochemical study on the stems and leaves of this species resulted in the isolation of 15 new PPAPs, hyperforatin A (**1**), 32-*epi*-hyperforatin A (**2**), hyperforatins B−D (**3**−**5**), 15-*epi*-hyperforatin D (**6**), hyperforatin E (**7**), 32-*epi*-hyperforatin E (**8**), hyperforatins F−I (**9**−**12**), 15-*epi*-hyperforatin I (**13**), and hyperforatins J−K (**14**−**15**), along with the known furohyperforin (**16**).[18] Herein, the isolation and structural determination of **1**−**15** and their biological activities are discussed.

RESULTS AND DISCUSSION

The molecular formula of hyperforatin A (**1**) was established as $C_{35}H_{52}O_6$ by the ^{13}C NMR data and a protonated HRESIMS molecular ion at m/z 569.3860 $[M + H]^+$, corresponding to 10 indices of hydrogen deficiency. The absorption bands at 1722 and 3440 cm^{-1} in the IR spectrum of **1** suggested the presence of carbonyl and hydroxy groups. The ^1H NMR data (Table 3) exhibited the signals of two olefinic protons (δ_H 4.96 and 5.00), an isopropyl group (δ_H 1.12, 3H; 1.06, 3H; 2.58, 1H), and eight methyls (δ_H 1.12−1.69, s). The ^{13}C NMR data (Table 1) indicated that **1** possesses 35 carbons comprising seven quaternary carbons, three carbonyls, two oxygenated tertiary carbons, and six methine, seven methylene, and 10 methyl

Received: December 23, 2016
Published: April 26, 2017

ACS Publications © 2017 American Chemical Society and American Society of Pharmacognosy

DOI: 10.1021/acs.jnatprod.6b01178
J. Nat. Prod. 2017, 80, 1493−1504

Chart 1

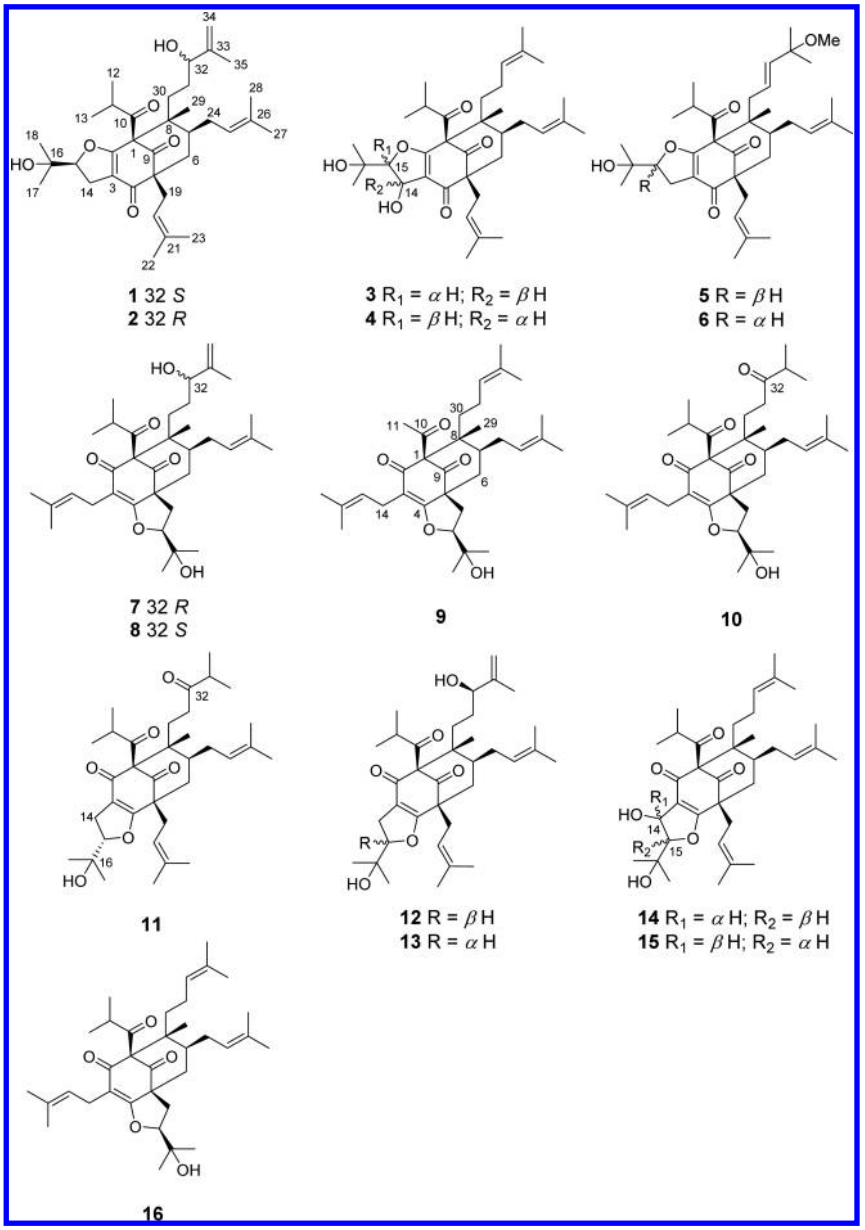

groups. On the basis of literature comparisons,[19] some of the signals were assigned to an enolized 1,3-diketo group (δ_C 174.2, C-2; 121.7, C-3; 192.7, C-4), two unconjugated carbonyl carbons (δ_C 206.9, C-9; 210.3, C-10), a methylene (δ_C 41.2, C-6), a methine (δ_C 44.2, C-7), and three quaternary carbons at δ_C 75.2 (C-1), 65.0 (C-5), and 48.9 (C-8). The aforementioned characteristic NMR data suggested that **1** is a PPAP derivative possessing a bicyclo[3.3.1]nonane core.[20]

An inspection of the 2D NMR spectra (including HSQC, HMBC, ^{1}H−^{1}H COSY, and NOESY) of **1** revealed that the structure of **1** is closely related to the furohyperforin isomer 2,[19] except for the C-8 side chain (C-30−C-35). The C-30 substituent of **1** was defined as a 3-methyl-3-buten-2-ol unit rather than a prenyl group in furohyperforin isomer 2. This conclusion was evidenced by the ^{1}H−^{1}H COSY interactions of H-30/H-31/H-32 and was supported by the HMBC interactions (Figure 1) from H_2-34 (δ_H 4.86 and 4.78) and Me-35 (δ_H 1.69) to C-32 (δ_C 77.8) and C-33 (δ_C 148.4) and from H-32 (δ_H 3.84) to C-30 (δ_C 35.6) and C-31 (δ_C 31.9). The relative configuration was assigned based on the NOESY data (Figure 1) and by comparison of the ^{13}C NMR chemical shifts of **1** with a structurally related PPAP derivative, garcinielliptone L (Table S1, Supporting Information).[21] The NOESY cross-peaks of H-6β (δ_H 1.41) with H-19, of Me-29 with H-6β, and of H-24 with Me-29 show that the C-1, C-5, C-7, and C-8 relative configurations of **1** are consistent with those of furohyperforin isomer 2.[19] The α-oriented H-15 in **1** was affirmed through the NOESY interactions of H-11 with Me-17 and Me-18.

32-*epi*-Hyperforatin A (**2**) had the same molecular formula as **1** according to its HRESIMS spectrum (m/z 569.3851 [M + H]$^+$). A comparison of the NMR data of **2** and **1** suggested that both compounds share the same 2D structure and relative configurations except for C-32. To confirm the absolute configurations of **1** and **2**, a suitable crystal of **2** was obtained. The subsequent crystallographic analysis (Figure 2) by Cu Kα radiation [CCDC 1532233, Flack parameter, −0.03(6)][22] permitted the unambiguous assignment of the absolute

DOI: 10.1021/acs.jnatprod.6b01178
J. Nat. Prod. 2017, 80, 1493−1504

Table 1. ^{13}C NMR (100 MHz) Data for 1−8 in Methanol-d_4 (δ in ppm)

no.	1	2	3	4	5	6	7	8
1	75.2	75.1	75.4	76.6	75.9	75.0	84.5	84.5
2	174.2	174.1	175.4	176.9	174.2	173.9	194.6	194.7
3	121.7	121.8	124.3	124.1	121.4	121.7	117.6	117.6
4	192.7	192.7	192.4	192.6	192.9	192.7	176.0	176.0
5	65.0	65.0	65.4	65.0	64.7	65.1	61.0	61.0
6	41.2	41.1	41.5	40.8	41.5	41.6	39.1	39.1
7	44.2	43.5	42.7	45.6	45.7	44.2	43.4	44.4
8	48.9	48.8	49.8	48.4	49.1	49.4	49.3	49.2
9	206.9	207.0	206.9	207.2	207.1	206.9	205.9	205.8
10	210.3	210.3	210.3	210.3	210.2	210.0	211.5	211.5
11	42.0	42.0	42.0	41.9	42.0	42.1	43.0	43.0
12	21.6	21.6	21.7	21.14	21.2	21.64	21.9	21.8
13	21.5	21.5	21.6	21.12	21.1	21.57	20.8	20.8
14	27.1	27.2	70.9	70.3	27.2	27.2	23.0	23.0
15	95.7	95.6	102.5	102.5	95.1	95.7	122.7	122.6
16	71.4	71.5	71.2	71.5	71.7	71.5	133.2	133.2
17	26.6	26.6	26.6	26.2	26.4	26.4	26.1	26.1
18	26.22	26.2	26.0	25.9	26.0	26.1	18.05	18.06
19	30.4	30.4	30.2	30.3	30.3	30.4	30.8	30.8
20	120.9	120.9	121.1	121.0	120.9	120.9	92.1	92.1
21	134.8	134.9	134.7	134.8	134.9	134.9	71.3	71.3
22	26.15	26.1	26.2	26.1	26.23	25.9	26.2	26.2
23	18.2	18.2	18.2	18.2	18.2	18.21	25.5	25.5
24	29.0	28.9	29.2	28.9	29.1	29.0	28.1	28.0
25	123.6	123.5	123.6	123.8	123.7	123.7	123.5	123.5
26	134.5	134.5	134.2	134.2	134.4	134.4	134.5	134.5
27	26.0	26.0	25.95	25.8	25.92	25.9	25.9	25.9
28	18.1	18.1	18.1	18.0	18.1	18.17	18.14	18.12
29	14.6	15.3	15.0	12.5	13.2	14.5	15.5	14.6
30	35.6	34.9	39.3	39.6	42.6	42.3	33.8	34.1
31	31.9	31.1	25.5	26.8	130.1	128.9	31.8	32.5
32	77.8	77.6	125.6	125.8	137.7	138.4	77.7	77.8
33	148.4	148.4	132.4	132.2	76.6	76.5	148.7	148.8
34	112.0	112.0	25.9	26.0	26.15	26.7	111.6	111.5
35	17.2	17.5	17.9	17.9	25.90	26.3	17.7	17.6
OMe					50.7	50.7		

configuration of **2** as (1*S*,5*R*,7*S*,8*R*,15*S*,32*R*). The different resonances in the vicinity of C-32 in **1** and **2** suggested a different C-32 absolute configuration. This was confirmed by opposite Cotton effects at 350 nm[23] (Figure S1, Supporting Information) of the in situ [$Rh_2(OCOCF_3)_4$] complex-induced electronic circular dichroism (ECD) spectra. Therefore, the structure of compound **2** is defined as the C-32 epimer of **1**.

Hyperforatins B (**3**) and C (**4**) share a molecular formula of $C_{35}H_{52}O_6$ based on their HRESIMS spectra. The similarities in the NMR spectra of **3** and **4** implied that the 2D structures of **3** and **4** are identical. Comparison of the NMR spectra of **3** and **4** with furohyperforin isomer 2 revealed that they are 14-hydroxy derivatives of furohyperforin isomer 2.[19] This was confirmed via the deshielded chemical shifts of C-14 (δ_C 70.9 in **3**; δ_C 70.3 in **4**) and the HMBC interactions of H-14 with C-2, C-4, and C-16. Moreover, compounds **3** and **4** had molecular masses 16 amu more than furohyperforin isomer 2 according to the HRESIMS data. The relative configurations of **3** and **4** at C-1, C-5, C-7, and C-8 were established to be the same as those of furohyperforin isomer 2[19] via the NOESY interactions of H-6β (δ_H 1.43 in both **3** and **4**) with H-19 and of Me-29 with H-24 and H-6β. Subsequently, H-14 and H-15 of compound **3** were concluded to be β- and α-oriented, respectively, according to the NOESY correlations from both H-11 (δ_H 2.61) and H-14 (δ_H 5.37) to Me-17 and Me-18. In contrast, the NOESY interactions of H-15 (δ_H 4.34) with Me-13 and of H-14 (δ_H 5.36) with Me-17 and Me-18 suggested that the orientations of H-14 and H-15 in **4** were the opposite of those in **3**.

Hyperforatin D (**5**) was isolated as a colorless oil. The molecular formula was established as $C_{36}H_{54}O_6$ via the ^{13}C NMR and HRESIMS data. The NMR data of **5** resembled those of **1**, except that the C-30 side chain was a (1*E*)-3-methoxy-3-methyl-1-buten-1-yl moiety in **5** rather than the 3-methyl-3-buten-2-ol group in **1**. This conclusion was supported by the $^1H-^1H$ COSY interactions of H-30/H-31/H-32 and the HMBC cross-peaks of Me-34 and Me-35 with C-32 and C-33 and the interactions of methoxy protons (δ_H 3.16) with C-33. Additionally, the large $^3J_{31,32}$ value of 16.0 Hz suggested that the $\Delta^{31(32)}$ double bond was *E*-configured. The relative configurations of the stereogenic centers at C-1, C-5, C-7, and C-8 in **5** were consistent with those of **1** based on the NOESY data (Figure S4, Supporting Information). The β-oriented H-15 in **5** was verified by the NOESY correlations of H-15 with H-11, Me-12, and Me-13.

15-*epi*-Hyperforatin D (**6**) was isolated as optically active colorless crystals with a molecular formula of $C_{36}H_{54}O_6$, as

DOI: 10.1021/acs.jnatprod.6b01178
J. Nat. Prod. 2017, 80, 1493−1504

Table 2. ^{13}C NMR (100 MHz) Data for 9−15 in Methanol-d_4 (δ in ppm)

no.	9	10	11	12	13	14	15
1	83.8	84.1	84.4	84.8	84.9	85.3	85.3
2	195.1	194.8	189.4	189.4	189.3	189.2	189.3
3	117.8	117.7	119.7	119.6	120.0	122.9	123.1
4	176.5	176.1	180.0	179.8	179.9	181.4	180.9
5	61.1	61.0	56.3	56.3	55.9	56.2	56.1
6	38.8	39.0	39.1	39.1	39.2	39.3	39.6
7	43.2	43.1	43.6	43.8	43.8	43.7	42.7
8	49.2	49.0	49.1	49.3	48.9	49.4	49.6
9	205.3	205.6	207.4	207.6	207.5	207.4	207.5
10	203.4	211.6	211.6	211.4	211.4	211.4	211.3
11	30.5	43.1	43.4	43.3	43.3	43.3	43.4
12		21.9	21.8	21.8	21.8	21.9	21.9
13		20.8	20.9	20.9	20.9	20.9	21.0
14	23.0	23.0	28.0	28.0	27.6	71.0	71.2
15	122.6	122.7	94.4	94.4	95.1	102.2	102.4
16	133.4	133.4	72.2	72.2	72.3	71.4	71.5
17	25.9	26.0	25.1	25.0	25.5	25.3	25.8
18	18.1	18.09	24.3	24.3	24.6	24.6	24.8
19	30.5	30.7	30.0	30.0	29.9	29.7	29.9
20	92.3	92.2	119.6	119.7	120.6	119.7	120.7
21	71.2	71.3	136.0	135.9	135.4	135.9	135.3
22	26.3	26.2	26.2	26.2	26.1	26.2	26.1
23	25.5	25.5	18.2	18.2	18.23	18.2	18.1
24	28.1	27.9	28.2	28.4	28.4	28.4	28.7
25	123.4	123.3	123.5	123.8	123.6	123.6	123.6
26	134.6	134.7	134.5	134.4	134.6	134.3	134.3
27	25.9	26.1	26.0	26.0	26.0	26.0	25.9
28	18.0	18.06	18.0	18.1	18.15	18.0	18.2
29	15.1	15.6	14.9	14.8	14.7	14.5	14.7
30	37.5	31.3	31.7	34.0	34.0	37.8	37.7
31	25.5	37.9	37.9	31.9	32.0	25.85	25.7
32	125.8	217.5	217.5	77.7	77.7	125.8	125.9
33	132.0	42.0	42.0	148.5	148.6	132.0	131.9
34	26.1	18.7	18.7	111.9	111.9	25.9	26.0
35	17.9	18.6	18.6	17.2	17.3	17.8	17.9

established by the HRESIMS and ^{13}C NMR data. Analysis of the NMR data of **5** and **6** (Tables 1, 3, and 4) implied that both compounds possess the same 2D structures. The only difference between the structures of **5** and **6** was the orientation of H-15. The NOESY interactions (Figure 4) from H-11 to Me-17 and Me-18 indicated that H-15 in **6** was α-oriented rather than the β-oriented in **5**. A suitable crystal of **6** was obtained, and subsequent X-ray diffraction analysis (Figure 3) was performed using Cu Kα radiation [CCDC 1523041, Flack parameter, 0.03(5)],[22] which permitted definition of the absolute configuration of **6** as (1*S*,5*R*,7*S*,8*R*,15*S*). Consequently, the absolute configurations of compounds **1**−**5** were confirmed by comparing their experimental ECD spectra with that of compound **6** (Figure 5).

The molecular formula of hyperforatin E (**7**), $C_{35}H_{52}O_6$, was determined by HRESIMS ([M + H]$^+$ *m*/*z* 569.3857). The NMR data of **7** indicated the presence of a 2,2,3,3,5-pentasubstituted tetrahydrofuran ring (δ_C 176.0, 61.0, 30.8, and 92.1), a hydroxyisopropyl group (δ_C 71.3, C-21; 26.2, Me-22; 25.5, Me-23), and a terminal double bond (δ_C 148.7, C-33; 111.6, C-34), which suggested that compound **7** is also an analogue of **1**. Inspection of the 2D NMR data of **7** showed that the difference between **7** and **1** involved the substitution pattern of the tetrahydrofuran ring. The $^1H-^1H$ COSY interaction of H-19/H-20 and the HMBC cross-peaks (Figure 4) from H-19 (δ_H 2.62 and 1.86) to C-6, C-9, and C-21 suggested the incorporation of the tetrahydrofuran ring across C-4 and C-5 of the bicyclic ring system in **7**. Subsequently, the NOESY interactions (Figure 4) of Me-29 with H-6β (δ_H 1.39) and H-24 and of H-6β with H-19 suggested that the relative configuration of compound **7** resembled those of furohyperforin (**16**).[18] In addition, H-20 of **7** was defined as α-oriented by the NOESY interaction (Figure 4) of H-20 (δ_H 4.66) with H-6α (δ_H 2.10). The 32*R* configuration of **7** was confirmed by the Cotton effect (Figure S2, Supporting Information) in the in situ [$Rh_2(OCOCF_3)_4$] complex-induced ECD[23] spectrum. Finally, the absolute configuration of **7** was unequivocally confirmed by X-ray crystallography[22] (Figure 6, CCDC 1523036) and ECD calculations (Figure S140, Supporting Information) and by comparing the experimental ECD curves of **7** (Figure 5) and **16**.[18]

32-*epi*-Hyperforatin E (**8**) and hyperforatin E (**7**) were separated by using chiral HPLC over a CHIRALPAK IC column. Comparisons of the HRESIMS, IR, UV, and NMR data of **8** and **7** suggested that both compounds possess the same 2D structure. The only difference between **8** and **7** was the orientation of H-32, as evidenced by the different carbon chemical shifts of C-30 (δ_C 34.1 in **8**; δ_C 33.8 in **7**) and C-31 (δ_C 32.5 in **8**; δ_C 31.8 in **7**). Additionally, compound **8** showed a positive E band in the in situ [$Rh_2(OCOCF_3)_4$] complex-induced ECD spectrum (Figure S2, Supporting Information), suggesting a 32*S* configuration in compound **8**.

Hyperforatin F (**9**) has the molecular formula $C_{33}H_{48}O_5$, as indicated by its HRESIMS spectrum ([M + H]$^+$ *m*/*z* 525.3547). Analysis of the NMR data of **9** indicated that the structure of **9** resembled that of furohyperforin (**16**),[18] except for the substituent at C-1. The 2-methyl-1-propanoyl moiety at C-1 of **16** was replaced by an acetyl moiety in **9**. This conclusion was supported not only by the HMBC interactions from Me-11 (δ 1.78) to C-10 and C-1 but also by the 28 amu lower molecular mass of **9** compared to **16**. Consequently, the NOESY cross-peaks of Me-29 with H-6β (δ 1.69), Me-11, and H-24 and of H-6β with H-19 suggested that **9** and **16** shared the same relative configurations.

The molecular formula of hyperforatin G (**10**), $C_{35}H_{52}O_6$, with a molecular mass of 16 amu higher than furohyperforin (**16**),[18] was evidenced by its ^{13}C NMR and HRESIMS data. Comparing the NMR data of **10** and **16** showed the presence of an additional carbonyl carbon at δ_C 217.5 in **10** and the absence of the $\Delta^{32(33)}$ double bond in **16**. These results and the HMBC cross-peaks of H-30 and Me-35 with C-32 (δ_C 217.5) suggested the presence of a carbonyl group at C-32 of **10**. Analysis of the NOESY data of **10** established that the configurations of all stereogenic centers of **10** resembled those of **16**[18] (Figure S4, Supporting Information). Furthermore, a comparison of the experimental ECD curves of **8**, **9**, and **10** (Figure 5) with that of **7** was used to define the absolute configurations of these compounds.

Hyperforatin H (**11**) possesses the molecular formula $C_{35}H_{52}O_6$, as established by the ^{13}C NMR and HRESIMS data. Comparing the NMR data of **11** (Tables 2 and 5) and furohyperforin isomer 1[19] suggested that the structure of **11** was similar to that of furhyperforin isomer 1, except for the substitution pattern at C-32. This observation was supported by the $^1H-^1H$ COSY cross-peak of H-30/H-31 and the HMBC interactions (Figure 4) of H-31, Me-34, and Me-35 with C-32.

DOI: 10.1021/acs.jnatprod.6b01178
J. Nat. Prod. 2017, 80, 1493−1504

Table 3. ^{1}H NMR (400 MHz) Data for Compounds 1−5 (δ in ppm, J in Hz)

no.	1[a]	2[a]	3[a]	4[a]	5[a]
6a	1.79 dd (12.8, 4.2)	1.78 dd (12.5, 4.0)	1.84 dd (13.6, 4.4)	1.73 overlap	1.78 dd (13.6, 4.2)
6b	1.41 t (12.8)	1.41 t (12.5)	1.43 t (13.6)	1.43 t (13.5)	1.39 t (13.6)
7	1.70[b]	1.70[b]	2.04 overlap	1.73 overlap	1.73 m
11	2.58 sept (6.5)	2.56 sept (6.5)	2.61 sept (6.5)	2.56 sept (6.5)	2.41 sept (6.5)
12	1.12 d (6.5)	1.13 d (6.5)	1.06 d (6.5)	1.07 d (6.5)	1.12 d (6.5)
13	1.06 d (6.5)	1.07 d (6.5)	1.13 d (6.5)	1.12 d (6.5)	1.08 d (6.5)
14a	2.96 dd	2.95 dd	5.37 d (4.9)	5.36 d (4.0)	3.05 dd (14.8, 9.2)
14b	(15.3, 10.5)	(15.3, 10.5)			2.90 dd (14.8, 10.4)
15	4.88[b]	4.86[b]	4.39 d (4.9)	4.34 d (4.0)	4.83 dd (10.4, 9.2)
17	1.32 s	1.32 s	1.32 s	1.31 s	1.31 s
18	1.24 s	1.24 s	1.30 s	1.28 s	1.24 s
19a	2.40 dd (14.9, 7.2)	2.40 dd (14.4, 7.1)	2.40 dd (15.0, 7.1)	2.44 dd (14.5, 7.7)	2.39[b]
19b				2.38 dd (14.5, 7.0)	
20	4.96 t (7.2)	4.98[b]	4.98 t (7.1)	5.08[b]	4.99 t (7.1)
22	1.61 s	1.61 s	1.61 s	1.63 s	1.62 s
23	1.67 s	1.67 s	1.67 s	1.67 s	1.67 s
24a	2.09 dd (12.9, 4.6)	2.08 m	2.09[b]	2.12 m	2.28 dd (12.4, 5.2)
24b	1.74[b]	1.72[b]	1.77[b]	1.72 overlap	1.66 overlap
25	5.00 m	5.01[b]	5.05 m	4.95 t (7.3)	4.97 m
27	1.69 s	1.68 s	1.67 s	1.65 s	1.66 s
28	1.58 s	1.58 s	1.58 s	1.55 s	1.56 s
29	1.12 s	1.11 s	1.14 s	1.09 s	1.09 s
30a	1.73[b]	1.64 overlap	1.72 m	1.91 dd (13.2, 4.7)	2.74 ddd (14.9, 6.2, 1.8)
30b	1.52[b]		1.61[b]	1.50 m	2.39 overlap
31a	1.60 m	1.59 overlap	2.05 overlap	2.20 m	5.76 ddd (16.0, 8.7, 6.2)
31b	1.53[b]		1.96 m	1.96 m	
32	3.84 t (6.1)	3.89 t (5.9)	5.02[b]	5.06[b]	5.44 br d (16.0)
34a	4.86 br s	4.88 br s	1.67 s	1.64 s	1.25 s
34b	4.78 br s	4.80 br s			
35	1.69 s	1.68 s	1.60 s	1.60 s	1.26 s
OMe					3.16 s

[a]Recorded in methanol-d_4. [b]Signal partially obscured.

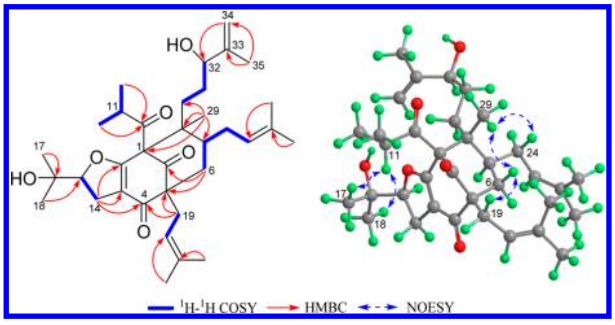

Figure 1. Key 2D NMR correlations of 1.

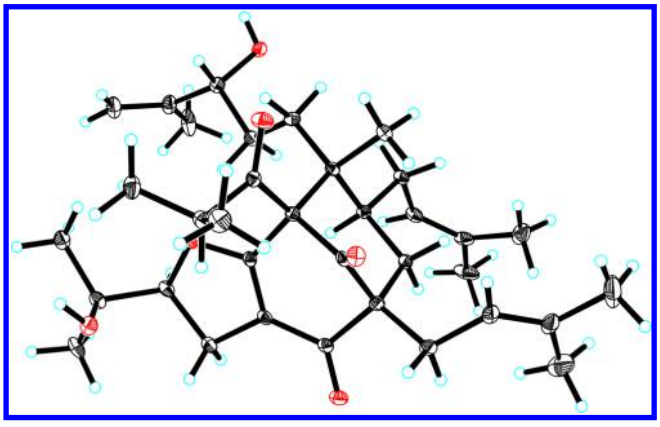

Figure 2. ORTEP drawing of compound 2.

The relative configurations at C-1, C-5, C-7, and C-8 of 11 were the same as those of furohyperforin isomer 1, as determined by the NOESY interactions of Me-29 with H-6β (δ 1.51) and H-24 and of H-6β with H-19 (Figure 4). Subsequently, the H-15β orientation was deduced from the NOESY interactions from Me-17 and Me-18 to H-6α and from Me-17 and Me-18 to H-25. The absolute configuration of 11 was defined as (1*R*,5*R*,7*S*,8*R*,15*S*) by comparison of the calculated and experimental ECD spectra (Figure 7). Compounds 10 and 11 are the first examples of natural [3.3.1]-type PPAPs with carbonyl functionality at C-32.

Both hyperforatin I (12) and 15-*epi*-hyperforatin I (13) possess the same molecular formula of $C_{35}H_{52}O_6$ based on their HRESIMS data. The analyses of their 1D NMR data (Tables 2 and 5) showed that both compounds contain a dihydrofuran moiety, a hydroxyisopropyl group, and a terminal double bond. Interpretation of their 2D NMR data indicated that the structures of 12 and 13 resembled that of compound 7, except for the substitution pattern of the dihydrofuran moiety. The HMBC cross-peaks of H-14 with C-3 and C-4 and the ^{1}H−^{1}H COSY interaction of H-14/H-15 demonstrated that the dihydrofuran moieties of compounds 12 and 13 were incorporated into the bicyclo[3.3.1]nonane core at C-3 and C-4 rather than at C-4 and C-5 as in compound 7. The relative configurations at C-1, C-5, C-7, and C-8 of 12 and 13 resemble

DOI: 10.1021/acs.jnatprod.6b01178
J. Nat. Prod. 2017, 80, 1493−1504

Table 4. ^{1}H NMR (400 MHz) Data for Compounds 6−10 (δ in ppm, J in Hz)

no.	6[a]	7[a]	8[a]	9[a]	10[a]
6a	1.79 dd (13.4, 3.9)	2.10 overlap	2.10 m	2.12 dd (12.8, 3.4)	2.15 br d (8.7)
6b	1.39 t (13.4)	1.65 overlap	1.65 overlap	1.69 overlap	1.68 overlap
7	1.70 overlap	1.66 overlap	1.65 overlap	1.75 overlap	1.66 overlap
11	2.55 sept (6.5)	1.99 sept (6.5)	2.00 sept (6.5)	1.78 s	2.01 overlap
12	1.13 d (6.5)	0.97 d (6.5)	0.96 d (6.5)		0.97 d (6.5)
13	1.08 d (6.5)	1.05 d (6.5)	1.04 d (6.5)		1.05 d (6.5)
14a	2.98 dd (15.5, 10.4)	3.10 dd (14.0, 7.9)	3.11 dd (14.0, 7.8)	3.10 dd (14.0, 7.6)	3.13 dd (14.0, 7.6)
14b		3.00 dd (14.0, 7.0)	3.01 dd (14.0, 7.0)	3.03 dd (14.0, 7.4)	3.02 dd (14.0, 7.2)
15	4.96[b]	5.15 t (7.5)	5.16 t (7.4)	5.18 t (7.4)	5.19 t (7.3)
17	1.33 s	1.65 s	1.65 s	1.65 s	1.67 s
18	1.25 s	1.71 s	1.72 s	1.72 s	1.73 s
19a	2.40 dd (14.5, 8.0)	2.62 dd (13.0, 10.8)	2.63 dd (13.0, 10.8)	2.63 dd (13.0, 10.8)	2.65 dd (13.0, 10.8)
19b		1.86 dd (13.0, 5.7)	1.86 dd (13.0, 5.6)	1.89 dd (13.0, 5.7)	1.89 dd (13.0, 5.6)
20	4.97[b]	4.66 dd (10.8, 5.7)	4.66 dd (10.8, 5.6)	4.70 dd (10.8, 5.7)	4.69 dd (10.8, 5.6)
22	1.61 s	1.34 s	1.34 s	1.35 s	1.35 s
23	1.67 s	1.21 s	1.21 s	1.21 s	1.21 s
24a	2.22 m	2.11 overlap	2.19 dd (14.1, 5.9)	2.12 overlap	2.08 dd (14.2, 6.0)
24b	1.70 overlap	1.77 m	1.77 m	1.80 m	1.78 m
25	4.95[b]	5.01 t (7.1)	5.02 t (7.1)	5.04 t (7.2)	5.02 t (7.2)
27	1.67 s	1.70 s	1.70 s	1.65 s	1.70 s
28	1.57 s	1.60 s	1.61 s	1.60 s	1.59 s
29	1.13 s	1.04 s	1.04 s	1.03 s	1.05 s
30a	2.49 m	1.90 m	1.84[b]	1.78 overlap	2.00 overlap
30b		1.59[b]	1.61 overlap	1.59 overlap	
31a	5.70 dt (15.7, 7.4)	1.57[b]	1.67[b]	1.96 m	2.55 m
31b			1.53 m		
32	5.42 br d (15.7)	3.88 t (6.1)	3.85 t (6.2)	5.00 t (7.1)	
33					2.64[b]
34a	1.24 s	4.90 br s	4.89 br s	1.67 s	1.07 d (6.9)
34b		4.79 br s	4.79 br s		
35	1.26 s	1.71 s	1.73 s	1.60 s	1.08 d (6.9)
OMe	3.16 s				

[a]Recorded in methanol-d_4. [b]Signal partially obscured.

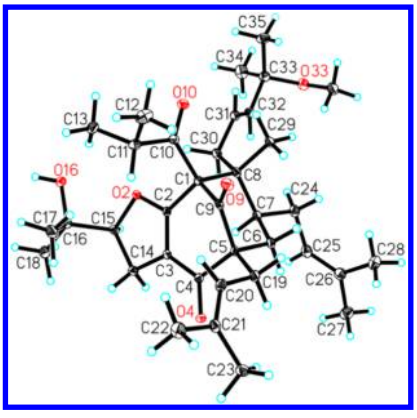

Figure 3. ORTEP drawing of compound 6.

those of compound 7 based on their NOESY data (Figure S4, Supporting Information). The 32R configurations of 12 and 13 were confirmed by negative Cotton effects in the in situ [$Rh_2(OCOCF_3)_4$] complex-induced ECD spectra (Figure S3, Supporting Information).[23] Subsequently, the only difference between 12 and 13 was the orientation of H-15. Its β orientation was established by the NOESY interactions from Me-17 and Me-18 to H-25. The H-15α orientation in 13 was deduced by the NOESY correlations from Me-17 and Me-18 to H-20. The C-1, C-5, C-7, and C-8 absolute configurations of 12 and 13 were defined as the same as those of 11 by comparison of their experimental ECD spectra with that of 11 (Figure 7).

The molecular formula for hyperforatins J (14) and K (15) was defined as $C_{35}H_{52}O_6$ by ^{13}C NMR and HRESIMS data. Analyses of their 1D NMR data demonstrated that the 2D structures of 14 and 15 resembled that of furohyperforin isomer 1,[19] except for the presence of a C-14 hydroxy functionality in 14 and 15. This assignment was confirmed by the ^{1}H−^{1}H COSY interaction of H-14/H-15 and the HMBC cross-peaks of H-14 with C-2 and C-4. The relative configurations of C-1, C-5, C-7, and C-8 were defined from the analyses of their NOESY data (Figure S4, Supporting Information). Moreover, the H-15β orientation of 14 was established by the NOESY cross-peaks from H-6α (δ_H 1.98) to Me-17 and Me-18. The H-14α orientation of 14 was confirmed by the NOESY interactions of H-14 (δ_H 5.21) with Me-17 and Me-18. For 15, the NOESY correlations from Me-18 to H-20 (δ_H 5.16) and from H-14 (δ_H 5.27) to Me-17 and Me-18 showed that the orientations of H-14 and H-15 were β and α, respectively. Therefore, the structures of 14 and 15 are defined as the 14-hydroxy derivatives of furohyperforin isomer 1.[19] In addition, the absolute configurations of 14 and 15 were confirmed by comparison with the experimental ECD spectra of 11 (Figure 7).

The definition of the absolute configuration of PPAPs is a challenge because of the multiple stereogenic centers in the

DOI: 10.1021/acs.jnatprod.6b01178
J. Nat. Prod. 2017, 80, 1493−1504

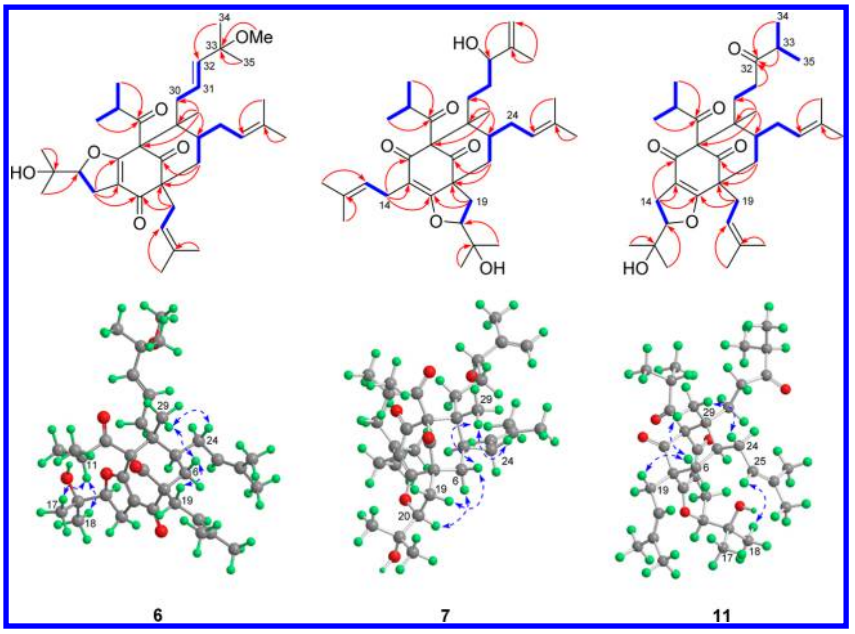

Figure 4. Key 2D NMR correlations of **6**, **7**, and **11**.

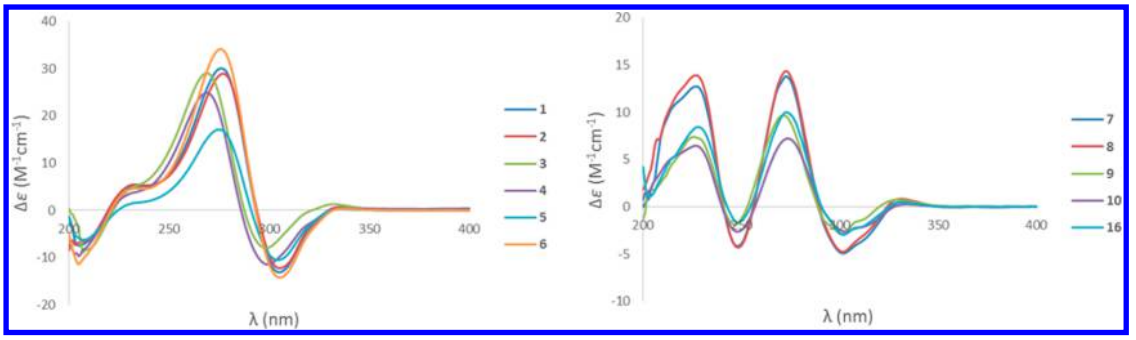

Figure 5. Experimental ECD (in MeOH) spectra of **1**–**6** (left) and **7**–**10** (right).

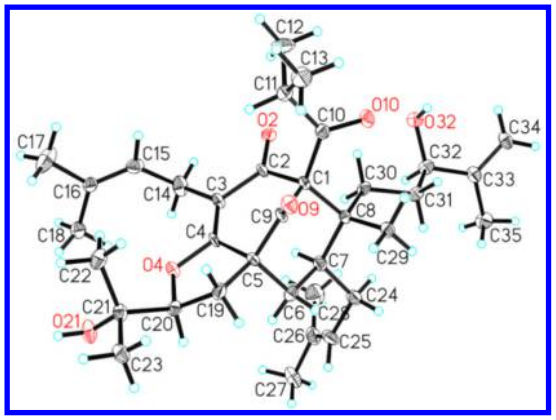

Figure 6. ORTEP drawing of compound **7**.

molecules and the difficulty of forming suitable crystals for crystallographic analysis. In this study, however, we implemented several methodologies, including experimental and calculated ECD, $Rh_2(OCOCF_3)_4$-induced ECD, and X-ray crystallography to successfully determine the absolute configurations of a series of PPAPs from the medicinally important plant *H. perforatum*. Hyperforatin F (**9**) is the first example of a PPAP containing a unique acetyl functionality at C-1. Although investigations on the biosyntheses of PPAPs have been previously reported,[24] the hypothetical pathway for the generation of **9** (Scheme 1) will provide new insights into PPAP biosynthesis.

Since several PPAPs have been reported to inhibit acetylcholinesterase (AChE),[25] all the new compounds, except for **7**, were tested for their AChE inhibitory activities (Table 6) using Ellman's method.[26] Compounds **3**, **5**, **6**, **8**, and **9** exhibited moderate AChE inhibitory activities with IC_{50} values of 8.83, 7.17, 3.98, 9.13, and 8.75 μM, respectively. Additionally, the cytotoxic activities of selected PPAPs were tested against a panel of human cancer cell lines, including HL-60, SW-480, A549, SMMC-7721, and MCF-7, and the immortalized noncancerous Beas-2B human bronchial epithelial cell line using the 3-(4,5-dimethylthiazol-2-yl)-5(3-carboxymethoxyphenyl)-2-(4-sulfopheny)-2*H*-tetrazolium (MTS) method.[27] Taxol and cisplatin (DDP) were used as positive controls. Compounds **9** and **12** exerted cytotoxic activities against the SMMC7721 cell line, with IC_{50} values of 10.0 and 9.1 μM, respectively (Table S2, Supporting Information).

Alzheimer's disease (AD) is a major threat to the health of the elderly population.[28] Unprecedented possibilities for drug development have been provided by advances in basic science and molecular diagnostics.[29] One practical strategy to satisfy the urgent need to develop new agents for AD is to delve into bioactive organic substances or lead compounds from plant-derived secondary metabolites.[30] In this case, this series of

DOI: 10.1021/acs.jnatprod.6b01178
J. Nat. Prod. 2017, 80, 1493−1504

Table 5. ^{1}H NMR (400 MHz) Data for Compounds 11−15 (δ in ppm, J in Hz)

no.	11[a]	12[a]	13[a]	14[a]	15[a]
6a	2.01 overlap	1.98 dd (13.5, 4.2)	1.92 dd (13.6, 4.2)	1.98 dd (13.2, 3.8)	1.98 dd (13.1, 4.5)
6b	1.51 t (12.9)	1.50 t (13.5)	1.49 t (13.6)	1.55 t (13.2)	1.52 t (13.1)
7	1.64 m	1.67 overlap	1.69 overlap	1.65 overlap	2.01 overlap
11	2.12 sept (6.5)	2.11 sept (6.5)	2.10 sept (6.5)	2.23 sept (6.5)	2.09 sept (6.5)
12	1.01 d (6.5)	1.00 d (6.5)	1.00 d (6.5)	1.03 d (6.5)	1.01 d (6.5)
13	1.09 d (6.5)	1.08 d (6.5)	1.08 d (6.5)	1.10 d (6.5)	1.08 d (6.5)
14a	2.97 dd (15.1, 10.3)	2.96 dd (15.1, 10.4)	3.00 dd (15.0, 10.6)	5.21 d (3.7)	5.27 d (3.4)
14b	2.90 dd (15.1, 8.1)	2.88 dd (15.1, 8.1)	2.91 dd (15.0, 7.9)		
15	4.83 dd (10.3, 8.1)	4.82 dd (10.4, 8.1)	4.88 overlap	4.39 d (3.7)	4.44 d (3.4)
17	1.25 s	1.25 s	1.23 s	1.25 s	1.26 s
18	1.23 s	1.21 s	1.23 s	1.22 s	1.20 s
19a	2.49[b]	2.52 dd (14.8, 6.6)	2.54 dd (15.3, 6.0)	2.57 dd (14.7, 7.0)	2.55 m
19b		2.46 dd (14.8, 7.9)	2.47 dd (15.3, 7.5)	2.50 dd (14.7, 7.6)	2.50 m
20	5.10 t (7.3)	5.10 t (7.3)	5.14 t (6.9)	5.16 t (7.0)	5.16 t (6.9)
22	1.67 s	1.67 s	1.67 s	1.68 s	1.67 s
23	1.70 s	1.70 s	1.69 s	1.70 s	1.68 s
24a	2.03 overlap	2.06[b]	2.10 overlap	2.09 dd (13.5, 5.8)	2.12[b]
24b	1.77 m	1.78 m	1.83 m	1.79[b]	1.86 m
25	5.01 t (7.2)	5.01 t (7.2)	5.03 t (7.2)	4.99 m	5.09 t (7.1)
27	1.67 s	1.67 s	1.70 s	1.67 s	1.71 s
28	1.57 s	1.58 s	1.59 s	1.56 s	1.59 s
29	1.01 s	0.98 s	1.05 s	1.00 s	1.00 s
30a	1.93 m	1.65 overlap	1.66 overlap	1.81[b]	1.79 m
30b				1.49[b]	1.62 m
31a	2.54 m	1.63[b]	1.63[b]	2.05[b]	2.07 overlap
31b		1.47[b]	1.48[b]	1.91 m	2.00 overlap
32		3.83 t (6.3)	3.84 t (5.9)	5.01 m	5.02 t (7.1)
33	2.64 sept (7.0)				
34a	1.07 d (7.0)	4.87 br s	4.88 br s	1.66 s	1.65 s
34b		4.79 br s	4.79 br s		
35	1.07 d (7.0)	1.70 s	1.70 s	1.60 s	1.60 s

[a]Recorded in methanol-d_4. [b]Signal partially obscured.

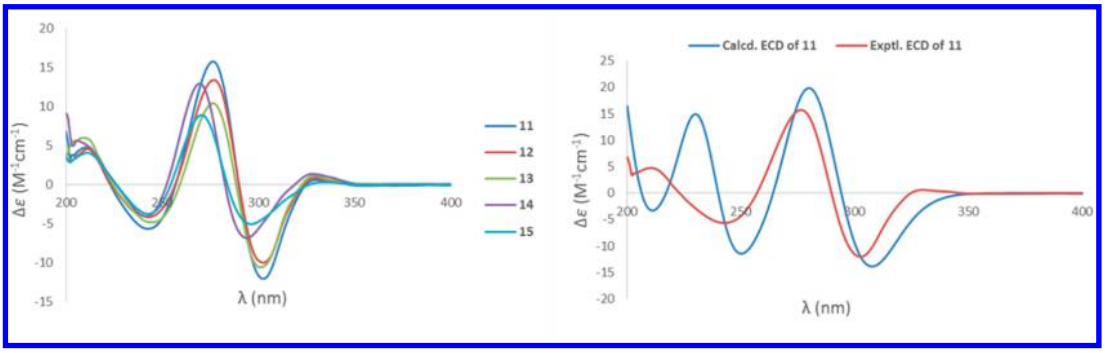

Figure 7. Experimental ECD (in MeOH) spectra of 11−15 (left) and calculated ECD spectra of 11 (right).

hyperforin analogues isolated from *H. perforatum* exerted AChE inhibitory activities, suggesting that these structurally diverse and bioactive PPAPs may be useful for the development of antineurodegenerative agents for AD.

EXPERIMENTAL SECTION

General Experimental Procedures. Melting points were obtained using an X-5 microscopic melting point apparatus (Beijing Tech, China), and optical rotations were recorded on a PerkinElmer 341 polarimeter (PerkinElmer Inc., Fremont, CA, USA). UV spectra were obtained in MeOH on a Lambda 35 instrument (PerkinElmer Inc.). ECD spectra were measured on a JASCO-810 spectrometer (JASCO, Tokyo, Japan). IR spectra were measured from a Vertex 70 FT-IR spectrophotometer (Bruker, Karlsruhe, Germany). The NMR spectra were measured on a Bruker AM-400 spectrometer, and the chemical shifts were referenced to the signals of residual peaks for methanol-d_4 (δ_C 49.0 and δ_H 3.31) and $CDCl_3$ (δ_C 77.0 and δ_H 7.26). HRESIMS data were obtained with a Bruker MicrOTOF II spectrometer (Bruker, Germany). Semipreparative HPLC was performed on a Dionex HPLC system using a reversed-phase (RP) C_{18} column (10 × 250 mm), an Ultimate SiO_2 column (10 × 250 mm), and a CHIRALPAK IC column (4.6 × 250 mm). Column chromatography (CC) was performed using MCI gel (75−150 μm, Merck, Germany), ODS (50 μm, YMC Co. Ltd., Japan), silica gel (200−300, 100−200, and 80−120 mesh; Qingdao Marine Chemical Inc., China), and Sephadex LH-20 (Pharmacia Biotech AB, Uppsala, Sweden).

DOI: 10.1021/acs.jnatprod.6b01178
J. Nat. Prod. 2017, 80, 1493−1504

Scheme 1. Possible Biosynthesis Pathway of Hyperforatin F (9)

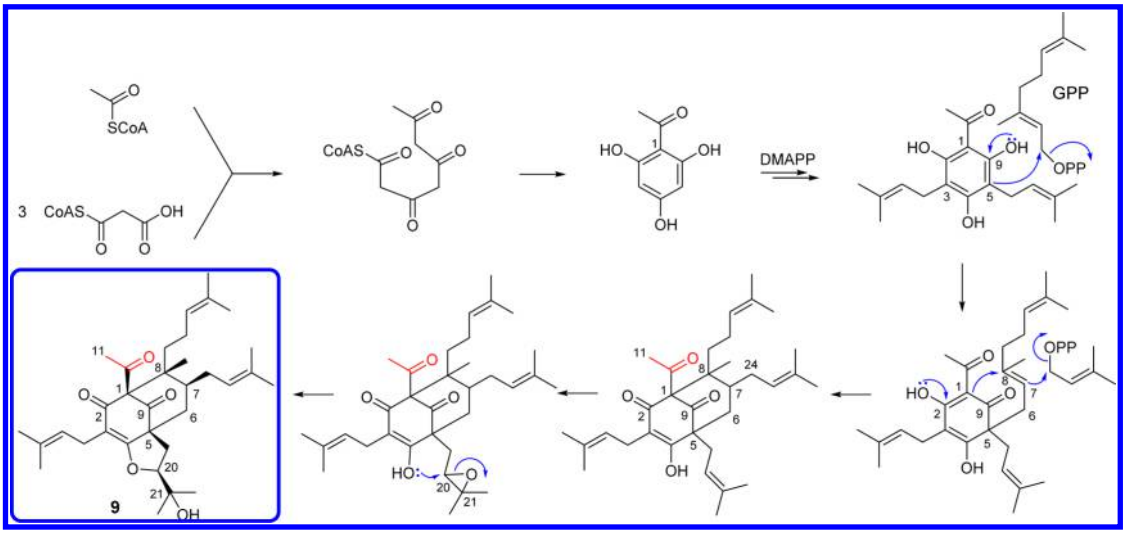

Table 6. Acetylcholinesterase Inhibitory Activity with IC_{50} Values (μM)

	1	2	3	4	5	6	8	9	10	11	12	13	14	15	TA[a]
IC_{50} (μM)	10.72	19.60	8.83	12.55	7.17	3.98	9.13	8.75	24.26	10.88	26.43	25.07	18.55	11.26	0.27
SD (μM)	0.732	0.850	0.599	1.392	0.134	0.924	1.022	0.521	1.673	1.422	5.561	3.436	2.588	0.341	0.013

[a]Tacrine was used as positive control.

Plant Material. The stems and leaves of *H. perforatum* were collected from the Muyu Town in the Shennongjia District (Hubei Province, People's Republic of China) in August 2014. The plants were identified by Prof. C. G. Zhang of the Huazhong University of Science and Technology (HUST). A voucher specimen (no. HP20140826) was deposited in the Tongji Medical College, HUST.

Extraction and Isolation. The air-dried stems and leaves of *H. perforatum* (105 kg) were soaked in 95% EtOH (3 × 105 L) to afford a residue under vacuum, and the crude extract was sequentially suspended in H_2O and partitioned with CH_2Cl_2. The CH_2Cl_2 fraction (3.8 kg) was separated by silica gel CC (100−200 mesh) using a gradient of petroleum ether−acetone (50:1−0:1) as the eluent to obtain seven fractions (A−G). Fr. C (203.0 g) was loaded onto an MCI gel column (MeOH−H_2O, 90−100%) to remove the pigment and subsequently loaded onto an RP C_{18} column (MeOH−H_2O, 50−100%) to yield eight subfractions, C1−C8. Fr. C5 (13.1 g) was loaded onto a silica gel column to yield 11 fractions (C5a−C5k) using petroleum ether−acetone (30:1−0:1). Fr. C5d (1.5 g) was loaded onto Sephadex LH-20 (MeOH), followed by RP HPLC, to yield **10** (10.6 mg, t_R 26.2 min, CH_3CN−H_2O, 60%) and by using chiral HPLC methods (*n*-hexane−EtOH, 95%) to yield **5** (6.4 mg, t_R 7.6 min) and **6** (4.5 mg, t_R 11.1 min). Fr. C5f (1.6 g) was separated using a process that was similar to the process used for Fr. C5d to yield **7** (3.0 mg, t_R 12.2 min, *n*-hexane−EtOH, 98%) and **8** (8.8 mg, t_R 14.3 min, *n*-hexane−EtOH, 98%). Compounds **1** (16.6 mg) and **2** (9.8 mg) were both separated from Fr. C5g (1.3 g) by Sephadex LH-20 (MeOH) and subsequently subjected to an RP C_{18} column (MeOH−H_2O, 50−85%) to yield five fractions (C5g1−C5g5) and finally purified from Fr. C5g3 by semipreparative HPLC (CH_3CN−H_2O, 90%, t_R 15.8 min, for **1**; *n*-hexane−EtOH, 95%, t_R 6.8 min for **2**). Subsequently, compounds **12** (5.2 mg) and **13** (4.3 mg) were separated from Fr. C5g4 by RP HPLC (MeOH−H_2O, 90%, t_R 20.2 min, for **12**; CH_3CN−H_2O, 95%, t_R 11.5 min, for **13**). Fr. C6 (19.23 g) was separated into eight fractions (C6a−C6h) by using a silica gel column with petroleum ether−EtOAc (30:1−0:1). Fr. C6d (2.74 g) was loaded onto an ODS RP-C_{18} column (MeOH−H_2O, 40−80%) and further purified by RP HPLC to afford **3** (26.3 mg, t_R 24.9 min, CH_3CN−H_2O, 95%), **4** (25.3 mg, t_R 30.1 min, CH_3CN−H_2O, 92%), **14** (34.2 mg, t_R 34.8 min, CH_3CN−H_2O, 90%), and **15** (27.5 mg, t_R 32.0 min, CH_3CN−H_2O, 92%). Fr. C6c (3.6 g) was separated on an ODS RP-C_{18} column (MeOH−H_2O, 60−90%) and RP HPLC to yield **9** (3.5 mg, t_R 13.0 min, CH_3CN−H_2O, 100%) and **11** (6.5 mg, t_R 12.6 min, CH_3CN−H_2O, 100%). Known compound **16** (21.4 mg) was obtained from Fr. C6b (4.53 mg) using an ODS RP-C_{18} column (MeOH−H_2O, 60−100%) and RP HPLC (t_R 34.5 min, CH_3CN−H_2O, 90%).

*Hyperforatin A (**1**):* colorless oil; $[\alpha]^{26}_D$ +84 (*c* 0.5, MeOH); UV (MeOH) λ_{max} (log ε) = 203 (4.10) and 281 (4.04) nm; ECD (MeOH) λ_{max} ($\Delta\varepsilon$) 205 (−7.45), 276 (+30.04), 305 (−13.11) nm; IR (KBr) ν_{max} 3440, 2973, 2929, 1722, 1643, 1616, 1446, 1383, 1236 cm^{-1}; 1D NMR data, Tables 1 and 3; HRESIMS *m*/*z* 569.3860 $[M + H]^+$ (calcd for $C_{35}H_{53}O_6$, 569.3842).

*32-epi-Hyperforatin A (**2**):* colorless crystals; mp 163−165 °C; $[\alpha]^{27}_D$ +78 (*c* 0.6, MeOH); UV (MeOH) λ_{max} (log ε) = 202 (4.20) and 281 (4.06) nm; ECD (MeOH) λ_{max} ($\Delta\varepsilon$) 203 (−7.31), 277 (+28.95), 305 (−12.23) nm; IR (KBr) ν_{max} 3445, 2976, 2925, 1725, 1662, 1620, 1454, 1383, 1236 cm^{-1}; 1D NMR data, Tables 1 and 3; HRESIMS *m*/*z* 569.3851 $[M + H]^+$ (calcd for $C_{35}H_{53}O_6$, 569.3842).

*Hyperforatin B (**3**):* colorless oil; $[\alpha]^{26}_D$ +106 (*c* 0.3, MeOH); UV (MeOH) λ_{max} (log ε) = 202 (4.23) and 273 (3.97) nm; ECD (MeOH) λ_{max} ($\Delta\varepsilon$) 207 (−8.84), 269 (+29.05), 299 (−7.95) nm; IR (KBr) ν_{max} 3437, 2974, 2929, 1724, 1642, 1616, 1446, 1384, 1226 cm^{-1}; 1D NMR data, Tables 1 and 3; HRESIMS *m*/*z* 569.3846 $[M + H]^+$ (calcd for $C_{35}H_{53}O_6$, 569.3842).

*Hyperforatin C (**4**):* colorless oil; $[\alpha]^{27}_D$ +12 (*c* 0.5, MeOH); UV (MeOH) λ_{max} (log ε) = 203 (4.54) and 272 (4.29) nm; ECD (MeOH) λ_{max} ($\Delta\varepsilon$) 205 (−9.69), 269 (+24.88), 299 (−11.44) nm; IR (KBr) ν_{max} 3434, 2974, 2929, 1725, 1648, 1616, 1445, 1384, 1234 cm^{-1}; 1D NMR data, Tables 1 and 3; HRESIMS *m*/*z* 569.3838 $[M + H]^+$ (calcd for $C_{35}H_{53}O_6$, 569.3842).

*Hyperforatin D (**5**):* colorless oil; $[\alpha]^{26}_D$ +12 (*c* 0.5, MeOH); UV (MeOH) λ_{max} (log ε) = 202 (4.41) and 280 (4.21) nm; ECD (MeOH) λ_{max} ($\Delta\varepsilon$) 207 (−6.24), 275 (+17.08), 304 (−10.51) nm; IR (KBr) ν_{max} 3437, 2975, 2930, 1722, 1656, 1621, 1445, 1383, 1243 cm^{-1}; 1D NMR data, Tables 1 and 3; HRESIMS *m*/*z* 605.3828 $[M + Na]^+$ (calcd for $C_{36}H_{54}O_6Na$, 605.3818).

*15-epi-Hyperforatin D (**6**):* colorless crystals; mp 108−110 °C; $[\alpha]^{26}_D$ +54 (*c* 0.6, MeOH); UV (MeOH) λ_{max} (log ε) = 202 (4.31) and 280 (4.29) nm; ECD (MeOH) λ_{max} ($\Delta\varepsilon$) 205 (−11.40), 276 (+34.12), 305 (−14.21) nm; IR (KBr) ν_{max} 3442, 2975, 2929, 1724,

DOI: 10.1021/acs.jnatprod.6b01178
J. Nat. Prod. 2017, 80, 1493−1504

1655, 1620, 1446, 1382, 1238 cm^{-1}; 1D NMR data, Tables 1 and 4; HRESIMS m/z 583.3992 $[M + H]^+$ (calcd for $C_{36}H_{55}O_6$, 583.3999).

Hyperforatin E (7): colorless crystals; mp 108−109 °C; $[\alpha]^{26}_D$ +66 (c 0.3, MeOH); UV (MeOH) λ_{max} (log ε) = 203 (4.42) and 273 (4.29) nm; ECD (MeOH) λ_{max} ($\Delta\varepsilon$) 227 (+12.73), 248 (−4.16), 273 (+13.80), 302 (−4.92) nm; IR (KBr) ν_{max} 3437, 2970, 2926, 1731, 1626, 1449, 1377, 1237, 1212 cm^{-1}; 1D NMR data, Tables 1 and 4; HRESIMS m/z 569.3857 $[M + H]^+$ (calcd for $C_{35}H_{53}O_6$, 569.3842).

32-epi-Hyperforatin E (8): colorless oil; $[\alpha]^{27}_D$ +81 (c 0.3, MeOH); UV (MeOH) λ_{max} (log ε) = 202 (4.27) and 273 (4.20) nm; ECD (MeOH) λ_{max} ($\Delta\varepsilon$) 227 (+13.92), 248 (−4.30), 273 (+14.36), 302 (−4.76) nm; IR (KBr) ν_{max} 3438, 2973, 2927, 1730, 1627, 1451, 1365, 1237, 1212 cm^{-1}; 1D NMR data, Tables 1 and 4; HRESIMS m/z 569.3836 $[M + H]^+$ (calcd for $C_{35}H_{53}O_6$, 569.3842).

Hyperforatin F (9): colorless oil; $[\alpha]^{22}_D$ +52 (c 0.4, MeOH); UV (MeOH) λ_{max} (log ε) = 202 (4.20) and 273 (4.01) nm; ECD (MeOH) λ_{max} ($\Delta\varepsilon$) 225 (+7.40), 247 (−1.90), 271 (+9.70), 301 (−2.86) nm; IR (KBr) ν_{max} 3449, 2971, 2925, 1730, 1622, 1451, 1366, 1237, 1209 cm^{-1}; 1D NMR data, Tables 2 and 4; HRESIMS m/z 525.3547 $[M + H]^+$ (calcd for $C_{33}H_{49}O_5$, 525.3580).

Hyperforatin G (10): colorless oil; $[\alpha]^{29}_D$ +48 (c 0.6, MeOH); UV (MeOH) λ_{max} (log ε) = 202 (4.05) and 273 (3.93) nm; ECD (MeOH) λ_{max} ($\Delta\varepsilon$) 227 (+6.47), 248 (−2.63), 273 (+7.23), 302 (−2.60) nm; IR (KBr) ν_{max} 3441, 2972, 2927, 1731, 1624, 1452, 1366, 1237, 1213 cm^{-1}; 1D NMR data, Tables 2 and 4; HRESIMS: m/z 569.3866 $[M + H]^+$ (calcd for $C_{35}H_{53}O_6$, 569.3842).

Hyperforatin H (11): colorless oil; $[\alpha]^{28}_D$ +34 (c 0.5, MeOH); UV (MeOH) λ_{max} (log ε) = 202 (4.10) and 283 (4.00) nm; ECD (MeOH) λ_{max} ($\Delta\varepsilon$) 242 (−5.64), 276 (+15.73), 302 (−12.03) nm; IR (KBr) ν_{max} 3442, 2972, 2929, 1729, 1623, 1408, 1384, 1236, 1182 cm^{-1}; 1D NMR data, Tables 2 and 5; HRESIMS m/z 569.3851 $[M + H]^+$ (calcd for $C_{35}H_{53}O_6$, 569.3842).

Hyperforatin I (12): colorless oil; $[\alpha]^{21}_D$ +23 (c 0.4, MeOH); UV (MeOH) λ_{max} (log ε) = 202 (4.12) and 282 (3.93) nm; ECD (MeOH) λ_{max} ($\Delta\varepsilon$) 243 (−4.16), 277 (+13.37), 302 (−9.97) nm; IR (KBr) ν_{max} 3434, 2972, 2927, 1727, 1614, 1447, 1409, 1382, 1236 cm^{-1}; 1D NMR data, Tables 2 and 5; HRESIMS m/z 591.3660 $[M + Na]^+$ (calcd for $C_{35}H_{52}O_6Na$, 591.3662).

15-epi-Hyperforatin I (13): colorless oil; $[\alpha]^{21}_D$ −28 (c 0.3, MeOH); UV (MeOH) λ_{max} (log ε) = 202 (4.20) and 282 (4.03) nm; ECD (MeOH) λ_{max} ($\Delta\varepsilon$) 244 (−4.79), 276 (+10.41), 301 (−10.55) nm; IR (KBr) ν_{max} 3435, 2960, 2925, 1726, 1617, 1451, 1408, 1382, 1230 cm^{-1}; 1D NMR data, Tables 2 and 5; HRESIMS m/z 591.3657 $[M + Na]^+$ (calcd for $C_{35}H_{52}O_6Na$, 591.3662).

Hyperforatin J (14): colorless oil; $[\alpha]^{27}_D$ +44 (c 0.5, MeOH); UV (MeOH) λ_{max} (log ε) = 202 (4.49) and 272 (4.30) nm; ECD (MeOH) λ_{max} ($\Delta\varepsilon$) 242 (−4.07), 269 (+12.90), 294 (−6.81) nm; IR (KBr) ν_{max} 3435, 2972, 2928, 1730, 1621, 1446, 1411, 1383, 1214 cm^{-1}; 1D NMR data, Tables 2 and 5; HRESIMS m/z 569.3860 $[M + H]^+$ (calcd for $C_{35}H_{53}O_6$, 569.3842).

Hyperforatin K (15): colorless oil; $[\alpha]^{27}_D$ −13 (c 0.5, MeOH); UV (MeOH) λ_{max} (log ε) = 202 (4.35) and 273 (3.97) nm; ECD (MeOH) λ_{max} ($\Delta\varepsilon$) 243 (−3.74), 270 (+8.89), 296 (−5.05) nm; IR (KBr) ν_{max} 3435, 2973, 2928, 1728, 1620, 1446, 1412, 1384, 1215 cm^{-1}; 1D NMR data, Tables 2 and 5; HRESIMS m/z 569.3832 $[M + H]^+$ (calcd for $C_{35}H_{53}O_6$, 569.3842).

X-ray Crystallographic Analysis. Crystals of **2**, **6**, and **7** were acquired from MeOH−H_2O. Intensity data were measured on a Bruker APEX DUO diffractometer outfitted with an APEX II CCD detector using Cu Kα radiation (λ = 1.541 78 Å) at 100 K. Data reduction and cell refinement were conducted with the Bruker SAINT program. The structures were determined by direct methods using SHELXS-97 (for details see the Supporting Information).[31]

Computational Methods. The conformations of compounds **7** and **11** were generated by BALLOON.[32] Quantum mechanical geometry optimizations of these conformations were performed using the semiempirical PM3 carried out by Gaussian 09 software,[33] and all the subsequent calculations used the same program. One of any two geometry-optimized conformations was identified as the same and removed when the root-mean-square (RMS) distance was less than 0.5 Å. Further optimization of the remaining conformations was conducted at the B3LYP/6-31G(d) level in MeOH with the IEFPCM solvation model, and duplicate conformations that occurred after these optimizations were neglected based on the same RMS distance criteria above. To confirm the stability of the final conformers, the harmonic vibrational frequencies were calculated. The ECD spectrum for each conformer was calculated at the B3LYP/6-311++G(d,p)//B3LYP/6-31G(d) level using the TDDFT methodology with MeOH as the solvent using the IEFPCM solvation model. The ECD spectrum for each conformer was modeled by a Gaussian function using a bandwidth σ of 0.5 eV. A UV correction was applied to each spectrum, and the final spectra were combined according to their Boltzmann weighting population contributions.[34]

Acetylcholinesterase Inhibitory Activity. The AChE inhibitory activities of the isolates were determined using Ellman's method[26] with a slight modification.

Cytotoxicity Assay. The cytotoxic effects of the isolates against HL-60, SW-480, A549, SMMC-7721, and MCF-7 were evaluated with the MTS method.[27]

■ ASSOCIATED CONTENT

Supporting Information

The Supporting Information is available free of charge on the ACS Publications website at DOI: 10.1021/acs.jnatprod.6b01178.

Original HRESIMS, IR, UV, 1D NMR, and 2D NMR data for all new compounds and the ECD spectra of the $[Rh_2(OCOCF_3)_4]$ complexes of compounds **1**, **2**, **7**, **8**, **12**, and **13**, (PDF)

X-ray crystallographic data of **2** (CIF)

For **6** (CIF)

For **7** (CIF)

■ AUTHOR INFORMATION

Corresponding Authors

*Tel: 86-27-82609207. E-mail: yongboxue@mail.hust.edu.cn. (Y. Xue).

*Tel: 86-27-83692311. Fax: 86-27-83691325. E-mail: zhangyh@mails.tjmu.edu.cn. (Y. Zhang).

ORCID

Junjun Liu: 0000-0001-9953-8633

Yongbo Xue: 0000-0001-9133-6439

Yonghui Zhang: 0000-0002-7222-2142

Notes

The authors declare no competing financial interest.

■ ACKNOWLEDGMENTS

We want to thank the Analytical and Testing Center of HUST for technological support. This research was financially assisted by the National Natural Science Foundation of China (Nos. 81641129, 31370372, and 81573316), the Fundamental Research Fund for the Central Universities (No. 2016YXMS149), the Program for New Century Excellent Talents in University, State Education Ministry of China (NCET-2008-0224), and the National Science and Technology Project of China (No. 2011ZX09102-004).

■ REFERENCES

(1) (a) Crockett, S. I.; Robson, N. K. B. *Plant Sci. Biotechnol.* **2011**, *5*, 1−13. (b) Rouis, Z.; Abid, N.; Aouni, M.; Faiella, L.; Dal Piaz, F.; De Tommasi, N.; Braca, A. *J. Nat. Prod.* **2013**, *76*, 979−982.

(2) Avato, P. In *Studies in Natural Products Chemistry*; Atta-ur-Rahman, Ed.; Elsevier: Amsterdam, 2005; Vol. *30*, pp 603−634.

(3) Shan, M. D.; Hu, L. H.; Chen, Z. L. *J. Nat. Prod.* **2001**, *64*, 127−130.
(4) (a) Schmitt, L. A.; Liu, Y.; Murphy, P. A.; Birt, D. F. *J. Agric. Food Chem.* **2006**, *54*, 2881−2890. (b) Wu, S. B.; Long, C.; Kennelly, E. J. *Nat. Prod. Rep.* **2014**, *31*, 1158−1174. (c) Wölfle, U.; Seelinger, G.; Schempp, C. M. *Planta Med.* **2014**, *80*, 109−120.
(5) Chatterjee, S. S.; Bhattacharya, S. K.; Wonnemann, M.; Singer, A.; Müller, W. E. *Life Sci.* **1998**, *63*, 499−510.
(6) (a) Müller, W. E.; Singer, A.; Wonnemann, M.; Hafner, U.; Rolli, M.; Schäfer, C. *Pharmacopsychiatry* **1998**, *31*, 16−21. (b) Whooley, M. A.; Simon, G. E. *N. Engl. J. Med.* **2000**, *343*, 1942−1950. (c) DiCarlo, G.; Borrelli, F.; Ernst, E.; Izzo, A. A. *Trends Pharmacol. Sci.* **2001**, *22*, 292−297. (d) Barnes, J.; Anderson, L. A.; Phillipson, J. D. *J. Pharm. Pharmacol.* **2001**, *53*, 583−600. (e) Bilia, A. R.; Gallori, S.; Vincieri, F. F. *Life Sci.* **2002**, *70*, 3077−3096. (f) Adam, P.; Arigoni, D.; Bacher, A.; Eisenreich, W. *J. Med. Chem.* **2002**, *45*, 4786−4793.
(7) (a) Gurevich, A. I.; Dobrynin, V. N.; Kolosov, M. N.; Popravko, S. A.; Riabova, I. D. *Antibiotiki* **1971**, *16*, 510−513. (b) Greeson, J. M.; Sanford, B.; Monti, D. A. *Psychopharmacology* **2001**, *153*, 402−414. (c) Hernández-López, J.; Crockett, S.; Kunert, O.; Hammer, E.; Schuehly, W.; Bauer, R.; Crailsheim, K.; Riessberger-Gallé, U. *Chem. Biodiversity* **2014**, *11*, 695−708.
(8) (a) Meruelo, D.; Lavie, G.; Lavie, D. *Proc. Natl. Acad. Sci. U. S. A.* **1988**, *85*, 5230−5234. (b) Lenard, J.; Rabson, A.; Vanderoef, R. *Proc. Natl. Acad. Sci. U. S. A.* **1993**, *90*, 158−162. (c) Kraus, G. A.; Melekhov, A.; Carpenter, S.; Wannemuhler, Y.; Petrich, J. *Bioorg. Med. Chem. Lett.* **2000**, *10*, 9−11.
(9) (a) Hammer, K. D.; Hillwig, M. L.; Solco, A. K.; Dixon, P. M.; Delate, K.; Murphy, P. A.; Wurtele, E. S.; Birt, D. F. *J. Agric. Food Chem.* **2007**, *55*, 7323−7331. (b) Cabrelle, A.; Dell'Aica, I.; Melchiori, L.; Carraro, S.; Brunetta, E.; Niero, R.; Scquizzato, E.; D'Intino, G.; Calzà, L.; Garbisa, S. *J. Leukocyte Biol.* **2008**, *83*, 212−219. (c) Süntar, I. P.; Akkol, E. K.; Yılmazer, D.; Baykal, T.; Kırmızıbekmez, H.; Alper, M.; Yeşilada, E. *J. Ethnopharmacol.* **2010**, *127*, 468−477.
(10) (a) Zou, Y.; Lu, Y.; Wei, D. *J. Agric. Food Chem.* **2004**, *52*, 5032−5039. (b) Sanchez-Reus, M. I.; Gomez del Rio, M. A.; Iglesias, I.; Elorza, M.; Slowing, K.; Benedi, J. *Neuropharmacology* **2007**, *52*, 606−616. (c) Carvalho, A. C.; Franklin, G.; Dias, A. C.; Lima, C. F. *Ind. Crops Prod.* **2014**, *59*, 177−183.
(11) (a) Hostanska, K.; Reichling, J.; Bommer, S.; Weber, M.; Saller, R. *Pharmazie* **2002**, *57*, 323−331. (b) Skalkos, D.; Stavropoulos, N. E.; Tsimaris, I.; Gioti, E.; Stalikas, C. D.; Nseyo, U. O.; Ioachim, E.; Agnantis, N. J. *Planta Med.* **2005**, *71*, 1030−1035.
(12) Gomez del Rio, M. A.; Sanchez-Reus, M. I.; Iglesias, I.; Pozo, M. A.; Garcia-Arencibia, M.; Fernandez-Ruiz, J.; Garcia-Garcia, L.; Delgado, M.; Benedi, J. *CNS Neurol. Disord.: Drug Targets* **2013**, *12*, 665−679.
(13) (a) Shimizu, Y.; Shi, S. L.; Usuda, H.; Kanai, M.; Shibasaki, M. *Angew. Chem., Int. Ed.* **2010**, *49*, 1103−1106. (b) Sparling, B. A.; Moebius, D. C.; Shair, M. D. *J. Am. Chem. Soc.* **2012**, *135*, 644−647. (c) Ting, C. P.; Maimone, T. J. *J. Am. Chem. Soc.* **2015**, *137*, 10516−10519.
(14) (a) Wonnemann, M.; Singer, A.; Müller, W. E. *Neuropsychopharmacology* **2000**, *23*, 188−197. (b) Schempp, C. M.; Kirkin, V.; Simon-Haarhaus, B.; Kersten, A.; Kiss, J.; Termeer, C. C.; Gilb, B.; Kaufmann, T.; Borner, C.; Sleeman, J. P. *Oncogene* **2002**, *21*, 1242−1250. (c) Gey, C.; Kyrylenko, S.; Hennig, L.; Nguyen, L. H. D.; Büttner, A.; Pham, H. D.; Giannis, A. *Angew. Chem., Int. Ed.* **2007**, *46*, 5219−5222.
(15) (a) Zhu, H.; Chen, C.; Yang, J.; Li, X. N.; Liu, J.; Sun, B.; Huang, S. X.; Li, D.; Yao, G.; Luo, Z.; Li, Y.; Zhang, J.; Xue, Y.; Zhang, Y. *Org. Lett.* **2014**, *16*, 6322−6325. (b) Zhu, H.; Chen, C.; Tong, Q.; Chen, X.; Yang, J.; Liu, J.; Sun, B.; Wang, J.; Yao, G.; Luo, Z.; Xue, Y.; Zhang, Y. *Sci. Rep.* **2015**, *5*, 14772. (c) Li, D.; Xue, Y.; Zhu, H.; Li, Y.; Sun, B.; Liu, J.; Yao, G.; Zhang, J.; Du, G.; Zhang, Y. *RSC Adv.* **2015**, *5*, 5277−5287. (d) Li, D.; Zhu, H.; Qi, C.; Xue, Y.; Yao, G.; Luo, Z.; Wang, J.; Zhang, J.; Du, G.; Zhang, Y. *Tetrahedron Lett.* **2015**, *56*, 1953−1955. (e) Zhu, H.; Chen, C.; Liu, J.; Sun, B.; Wei, G.; Li, Y.; Zhang, J.; Yao, G.; Luo, Z.; Xue, Y.; Zhang, Y. *Phytochemistry* **2015**, *115*, 222−230. (f) Zhu, H.; Chen, C.; Tan, D.; Li, D.; Guo, Y.; Wei, G.; Zhang, J.; Wang, J.; Luo, Z.; Xue, Y.; Zhang, Y. *RSC Adv.* **2016**, *6*, 86710−86716. (g) Zhu, H.; Chen, C.; Yang, J.; Li, D.; Zhang, J.; Guo, Y.; Wang, J.; Luo, Z.; Xue, Y.; Zhang, Y. *Tetrahedron* **2016**, *72*, 4655−4659.
(16) (a) Bann, C. M.; Parker, C. B.; Bradwejn, J.; Davidson, J. R.; Vitiello, B.; Gadde, K. M. *Depression Anxiety* **2004**, *20*, 114−122. (b) Martarelli, D.; Martarelli, B.; Pediconi, D.; Nabissi, M. I.; Perfumi, M.; Pompei, P. *Cancer Lett.* **2004**, *210*, 27−33. (c) Martínez-Poveda, B.; Quesada, A. R.; Medina, M. Á. *Int. J. Cancer* **2005**, *117*, 775−780.
(17) (a) Rücker, G.; Manns, D.; Hartmann, R.; Bonsels, U. *Arch. Pharm.* **1995**, *328*, 725−730. (b) Trifunović, S.; Vajs, V.; Macura, S.; Juranić, N.; Djarmati, Z.; Jankov, R.; Milosavljević, S. *Phytochemistry* **1998**, *49*, 1305−1310. (c) Verotta, L.; Appendino, G.; Jakupovic, J.; Bombardelli, E. *J. Nat. Prod.* **2000**, *63*, 412−415. (d) Shan, M. D.; Hu, L. H.; Chen, Z. L. *Chin. Chem. Lett.* **2000**, *11*, 701−704. (e) Vugdelija, S.; Vajs, V.; Trifunovic, S.; Djokovic, D.; Milosavljevic, S.; Ramdani, M.; Elidrissi, A.; Comte, O.; Genillard, S.; Nkubana, C. *Molecules* **2000**, *5*, M158. (f) Vajs, V.; Vugdelija, S.; Trifunović, S.; Karadzić, I.; Juranić, N.; Macura, S.; Milosavljević, S. *Fitoterapia* **2003**, *74*, 439−444. (g) Wu, J.; Cheng, X. F.; Harrison, L. J.; Goh, S. H.; Sim, K. Y. *Tetrahedron Lett.* **2004**, *45*, 9657−9659. (h) Charchoglyan, A.; Abrahamyan, A.; Fujii, I.; Boubakir, Z.; Gulder, T. A.; Kutchan, T. M.; Vardapetyan, H.; Bringmann, G.; Ebizuka, Y.; Beerhues, L. *Phytochemistry* **2007**, *68*, 2670−2677. (i) Hashida, C.; Tanaka, N.; Kashiwada, Y.; Ogawa, M.; Takaishi, Y. *Chem. Pharm. Bull.* **2008**, *56*, 1164−1167.
(18) Verotta, L.; Appendino, G.; Belloro, E.; Jakupovic, J.; Bombardelli, E. *J. Nat. Prod.* **1999**, *62*, 770−772.
(19) Lee, J. Y.; Duke, R. K.; Tran, V. H.; Hook, J. M.; Duke, C. C. *Phytochemistry* **2006**, *67*, 2550−2560.
(20) Ciochina, R.; Grossman, R. B. *Chem. Rev.* **2006**, *106*, 3963−3986.
(21) (a) Weng, J. R.; Tsao, L. T.; Wang, J. P.; Wu, R. R.; Lin, C. N. *J. Nat. Prod.* **2004**, *67*, 1796−1799. (b) Liu, X.; Yang, X. W.; Chen, C. Q.; Wu, C. Y.; Zhang, J. J.; Ma, J. Z.; Wang, H.; Yang, L. X.; Xu, G. *J. Nat. Prod.* **2013**, *76*, 1612−1618. (c) Yang, X. W.; Yang, J.; Xu, G. *J. Nat. Prod.* **2017**, *80*, 108−113.
(22) Flack, H. D. *Acta Crystallogr., Sect. A: Found. Crystallogr.* **1983**, *39*, 876−881.
(23) (a) Gerards, M.; Snatzke, G. *Tetrahedron: Asymmetry* **1990**, *1*, 221−236. (b) Frelek, J.; Szczepek, W. J. *Tetrahedron: Asymmetry* **1999**, *10*, 1507−1520.
(24) (a) Beerhues, L. *Phytochemistry* **2006**, *67*, 2201−2207. (b) Karppinen, K.; Hokkanen, J.; Tolonen, A.; Mattila, S.; Hohtola, A. *Phytochemistry* **2007**, *68*, 1038−1045. (c) Nualkaew, N.; Morita, H.; Shimokawa, Y.; Kinjo, K.; Kushiro, T.; De-Eknamkul, W.; Ebizuka, Y.; Abe, I. *Phytochemistry* **2012**, *77*, 60−69.
(25) (a) Butterweck, V. *CNS Drugs* **2003**, *17*, 539−562. (b) Griffith, T. N.; Varela-Nallar, L.; Dinamarca, M. C.; Inestrosa, N. C. *Curr. Med. Chem.* **2010**, *17*, 391−406. (c) Yang, X. W.; Deng, X.; Liu, X.; Wu, C. Y.; Li, X. N.; Wu, B.; Luo, H. R.; Li, Y.; Xu, H. X.; Zhao, Q. S.; Xu, G. *Chem. Commun.* **2012**, *48*, 5998−6000. (d) Yang, X. W.; Ding, Y.; Zhang, J. J.; Liu, X.; Yang, L. X.; Li, X. N.; Ferreira, D.; Walker, L. A.; Xu, G. *Org. Lett.* **2014**, *16*, 2434−2437.
(26) Ellman, G. L.; Courtney, K. D.; Andres, V. J.; Featherstone, R. M. *Biochem. Pharmacol.* **1961**, *7*, 88−95.
(27) (a) Reed, L. J.; Muench, H. *Am. J. Epidemiol.* **1938**, *27*, 493−497. (b) Malich, G.; Markovic, B.; Winder, C. *Toxicology* **1997**, *124*, 179−192.
(28) Nussbaum, R. L.; Ellis, C. E. *N. Engl. J. Med.* **2003**, *348*, 1356−1364.
(29) Scheltens, P.; Blennow, K.; Breteler, M. M.; de Strooper, B.; Frisoni, G. B.; Salloway, S.; Van der Flier, W. M. *Lancet* **2016**, *388*, 505−517.
(30) Newman, D. J.; Cragg, G. M. *J. Nat. Prod.* **2016**, *79*, 629−661.
(31) Sheldrick, G. M.; Schneider, T. R. *Methods Enzymol.* **1997**, *277*, 319−343.

DOI: 10.1021/acs.jnatprod.6b01178
J. Nat. Prod. 2017, 80, 1493−1504

(32) (a) Vainio, M. J.; Johnson, M. S. *J. Chem. Inf. Model.* **2007**, *47*, 2462−2474. (b) Puranen, J. S.; Vainio, M. J.; Johnson, M. S. *J. Comput. Chem.* **2010**, *31*, 1722−1732.
(33) Frisch, G. W. T. M. J.; Schlegel, H. B.; Scuseria, G. E.; Robb, M. A.; Cheeseman, J. R.; Scalmani, G.; Barone, V.; Mennucci, B.; Petersson, G. A.; Nakatsuji, H.; Caricato, M.; Li, X.; Hratchian, H. P.; Izmaylov, A. F.; Bloino, J.; Zheng, G.; Sonnenberg, J. L.; Hada, M.; Ehara, M.; Toyota, K.; Fukuda, R.; Hasegawa, J.; Ishida, M.; Nakajima, T.; Honda, Y.; Kitao, O.; Nakai, H.; Vreven, T.; Montgomery, J. A., Jr.; Peralta, J. E.; Ogliaro, F.; Bearpark, M.; Heyd, J. J.; Brothers, E.; Kudin, K. N.; Staroverov, V. N.; Kobayashi, R.; Normand, J.; Raghavachari, K.; Rendell, A.; Burant, J. C.; Iyengar, S. S.; Tomasi, J.; Cossi, M.; Rega, N.; Millam, J. M.; Klene, M.; Knox, J. E.; Cross, J. B.; Bakken, V.; Adamo, C.; Jaramillo, J.; Gomperts, R.; Stratmann, R. E.; Yazyev, O.; Austin, A. J.; Cammi, R.; Pomelli, C.; Ochterski, J. W.; Martin, R. L.; Morokuma, K.; Zakrzewski, V. G.; Voth, G. A.; Salvador, P.; Dannenberg, J. J.; Dapprich, S.; Daniels, A. D.; Farkas, Ö.; Foresman, J. B.; Ortiz, J. V.; Cioslowski, J.; Fox, D. J. *GAUSSIAN 09, Revision D.01*; Gaussian, Inc.: Wallingford, CT, 2009.
(34) Zhu, H. J. *Organic Stereochemsitry−Experimental and Computational Methods*; Wiley-VCH, Verlag GmbH & Co. KGaA: Weinheim, 2015.

DOI: 10.1021/acs.jnatprod.6b01178
J. Nat. Prod. 2017, 80, 1493−1504